BIOLOGY OF REPRODUCTION (2013) **89**(5):115, 1–12
Published online before print 2 October 2013.
DOI 10.1095/biolreprod.113.107995

Variation in Progesterone Receptors and GnRH Expression in the Hypothalamus of the Pregnant South American Plains Vizcacha, *Lagostomus maximus* (Mammalia, Rodentia)[1]

Verónica Berta Dorfman,[2,3,4] Lucía Saucedo,[3,4] Noelia Paula Di Giorgio,[5] Pablo Ignacio Felipe Inserra,[4] Nicolás Fraunhoffer,[4] Noelia Paola Leopardo,[4] Julia Halperín,[4] Victoria Lux-Lantos,[5] and Alfredo Daniel Vitullo[4]

[4]*Centro de Estudios Biomédicos, Biotecnológicos, Ambientales y Diagnóstico (CEBBAD), Universidad Maimónides, Ciudad Autónoma de Buenos Aires, Argentina*
[5]*Laboratorio de Neuroendocrinología, Instituto de Biología y Medicina Experimental (IByME)-CONICET, Ciudad Autónoma de Buenos Aires, Argentina*

ABSTRACT

In mammals, elevated levels of progesterone (P4) throughout gestation maintain a negative feedback over the hypothalamic-hypophyseal-gonadal (H-H-G) axis, avoiding preovulatory follicular growth and preventing ovulation. Recent studies showed that in the South American plains vizcacha (*Lagostomus maximus*) folliculogenesis progresses to preovulatory stages during gestation, and an ovulatory process seems to occur at midgestation. The aim of this work was to analyze hypothalamic gonadotropin-releasing hormone (GnRH) and P4 receptors (PR) expression and luteinizing hormone (LH) secretion and correlate these with the functional state of the ovary in nonovulating and ovulating females and gestating females with special emphasis in the supposedly ovulating females at midgestation. We investigated P4 and LH serum levels as well as the distribution, localization, and expression of PR and GnRH in the hypothalamus of *L. maximus* at different time points during gestation and in nongestating, ovulating and nonovulating, females. A significant increment in GnRH, P4, and LH was detected in midpregnant vizcachas with respect to early-pregnant and to ovulating females. PR was also significantly increased in midpregnant animals. PR was detected in neurons of the preoptic and hypothalamic areas. Coexistence of both PR and GnRH in neurons of medial preoptic area and supraoptic nucleus was detected. Midpregnant animals showed increased number of PR immunoreactive cells at median eminence, localized adjacently to GnRH immunoreactive fibers. High expression of hypothalamic GnRH and PR, despite an increased level of P4, was correlated with the presence of antral, preovulatory follicles, and luteinized unruptured follicles at midgestation that suggest a possible role of the H-H-G axis in the modulation of ovulation during gestation in *L. maximus*.

GnRH, hypothalamus, Lagostomus maximus*, ovary, plains vizcacha, progesterone, progesterone receptor*

INTRODUCTION

Pubertal development and adult reproductive function depend on the activation of the hypothalamic-hypophyseal-gonadal (H-H-G) axis. The gonadotropin-releasing hormone (GnRH), also known as luteinizing hormone-releasing hormone (LHRH), is the central regulator of fertility in mammals. It is involved in the modulation of the H-H-G axis. The ovarian progesterone (P4), which is able to diffuse across the blood-brain barrier into cells of the central nervous system, is an essential steroid hormone for the secretion of GnRH exerting its primary effect through the P4 receptors (PR). PR transcription in neurons that project to GnRH-secreting neurons activates via estradiol (E_2)-bound classical estrogen receptor alpha (ERα), which acts as a transcription factor on the PR promoter. Before ovulation, P4-bound PR may stimulate GnRH neurons acting directly as a transcription factor or by specific interactions with coregulator proteins [1, 2]. After ovulation, a progressive increase of P4 secretion from corpora lutea produces a negative feedback over GnRH secretion [3, 4]. In addition, P4 also acts in the pituitary gland by repressing luteinizing hormone (LH) expression in a receptor-dependent manner [5]. If fertilization takes place following ovulation, P4 levels increase progressively, modulating blastocyst implantation, and remain elevated throughout the ensuing pregnancy [6–8]. Elevated levels of P4 throughout gestation maintain the negative feedback over the H-H-G axis, arresting the final steps of folliculogenesis and preventing the formation of the preovulatory follicle and ovulation. At a variable time after delivery, depending on the species, cycling will be restored when P4 values drop down.

The neuroendocrinological picture briefly depicted above applies in general to all mammals in order to ensure gestation to term. Exceptionally, the South American plains vizcacha, *Lagostomus maximus*, has been reported to show preovulatory follicular formation and ovulation at midgestation [9–12]. This hystricognathe fossorial rodent inhabiting the Pampean region in Argentina [13] is a seasonal-breeder, medium-sized caviomorph showing many peculiar reproductive traits. Females are able to release up to 800 oocytes per estrous cycle, the highest ovulatory rate so far recorded for a mammal [9, 10]. The massive polyovulation seems to arise from the

[1]Supported by a PIP no. 0225–CONICET granted to V.B.D., a PICTO-CRUP no. 30972–ANPCyT (Agencia Nacional de Promoción Científica y Tencológica) granted to A.D.V., and by Fundación Científica Felipe Fiorellino, Universidad Maimónides, Argentina.
[2]Correspondence: Verónica Berta Dorfman, Centro de Estudios Biomédicos, Biotecnológicos, Ambientales y Diagnóstico (CEBBAD), Universidad Maimónides, Hidalgo 775 6to piso, C1405BCK, Ciudad Autónoma de Buenos Aires, Argentina.
E-mail: dorfman.veronica@maimonides.edu
[3]These authors contributed equally to this work.

Received: 27 February 2013.
First decision: 24 March 2013.
Accepted: 20 September 2013.

eISSN: 1529-7268 http://www.biolreprod.org
ISSN: 0006-3363

TABLE 1. Ovulation, pregnancy, and folliculogenesis status in *L. maximus* throughout the reproductive cycle.

Females	Ovulatory stigmata	Fetus or embryos	Corpus luteum[a]		Follicles[a,b]		
			1ry	2ry[c]	Primordial	1ry and 2ry	Antral
Nonovulating, nonpregnant	No	No	Yes[d]	No	+++	+	+
Ovulating	Yes	No	Yes	Yes	+++	+	++
Early pregnant	No	Yes	Yes	No	+++	++	+
Midpregnant	Yes	Yes	Yes	Yes	+++	+	++

[a] 1ry, primary corpora lutea; 2ry, secondary corpora lutea.
[b] Symbols indicate low (+), moderate (++), or high (+++) quantity of follicles per ovarian section.
[c] 2ry corpus luteum is easily distinguished since it retains the oocyte.
[d] Primary corpora lutea are occasionally found in nonovulating females.

unusual constitutive suppression of apoptosis in the *L. maximus* ovary that abolishes intraovarian oocyte demise through follicular atresia as in other mammals [11–14]. Folliculogenesis is not interrupted throughout the 155-day long-lasting pregnancy [11], leading to preovulatory follicular formation and the addition of secondary corpora lutea, increasing circulating P4 level that seems to take place around midgestation [12]. The neuroendocrine environment enabling preovulatory follicular formation that takes place at midgestation in *L. maximus* has not been so far investigated. We have recently described the general morphology and histology of the vizcacha hypothalamus and found a tissue organization comparable to other mammals [15]. In addition, we have shown that GnRH distribution in hypothalamic areas of the vizcacha brain is comparable to a variety of other mammalian species. However, GnRH surprisingly localizes also in the ventrolateral preoptic area of the vizcachas hypothalamus, where the supraoptic nucleus (SON) resides [15]. This unusual localization of GnRH in SON has only been previously reported in pig's brain [16], another well-known polyovulatory mammal. The aim of this work was to investigate hypothalamic GnRH and PR expression and LH secretion and correlate these observations with ovary functional state before and during gestation, paying special attention to midpregnancy. In order to further understand how the H-H-G axis is modulated in *L. maximus* to enable preovulatory follicular formation and luteinization at midgestation, we report here our analysis of LH, P4, and GnRH levels as well as a detailed analysis of the distribution, localization, and expression of PR in the hypothalamus of the vizcacha at different time points during gestation and its comparison to nongestating, both ovulating and nonovulating, females.

MATERIALS AND METHODS

Animals

Adult female plains vizcachas (2.5–3.0 kg body weight; 2.5–3 yr old, determined by the dry crystalline lens weight according to Jackson [17]) were captured from a resident natural population at the Estación de Cría de Animales Silvestres (ECAS), Villa Elisa, Buenos Aires province, Argentina. Animals were captured using live traps located at the entrance of burrows. All experimental protocols concerning animals were conducted in accordance with the Society for the Study of Reproduction's specific guidelines and standards, reviewed and authorized by the Institutional Committee on Use and Care of Experimental Animals from Universidad Maimónides, Argentina. Handling and killing of animals were performed in accordance with the National Institutes of Health Guidelines for the Care and Use of Laboratory Animals [18]. Appropriate procedures were performed to minimize the number of animals used. In order to obtain females at different reproductive stages, captures were planned according to the natural reproductive cycle previously described by Llanos and Crespo [19] and our own previous experience at field [11, 12, 14]. Nonovulating nonpregnant females (n = 15) were captured in December, ovulating females (n = 17) in February when reproductive season starts, early-pregnant females (n = 20) in April, and midpregnant females (n = 15) in July. Pregnancy was confirmed by the presence of visible implantation sites in early-pregnant animals or developing fetuses in midgestating females. The ovulatory status was assessed by ovary inspection for the presence of ovulatory stigmata at the time of killing. The presence of primary and secondary corpora lutea (luteinized, unruptured follicles) was assessed through ovary histological inspection in hematoxylin-eosin-stained sections. Secondary corpora lutea are easily recognized since they show oocyte retention in the luteinizing unruptured follicle as previously described by us [12]. On the basis of these criteria, females were categorized in the four groups indicated above, and the degree of follicular and corpora lutea development was established by the examination of histological cuts stained with hematoxylin-eosin (Table 1 and Fig. 1). Gestational age was estimated on the basis of capture time and fetal development as previously described by Leopardo et al. [14].

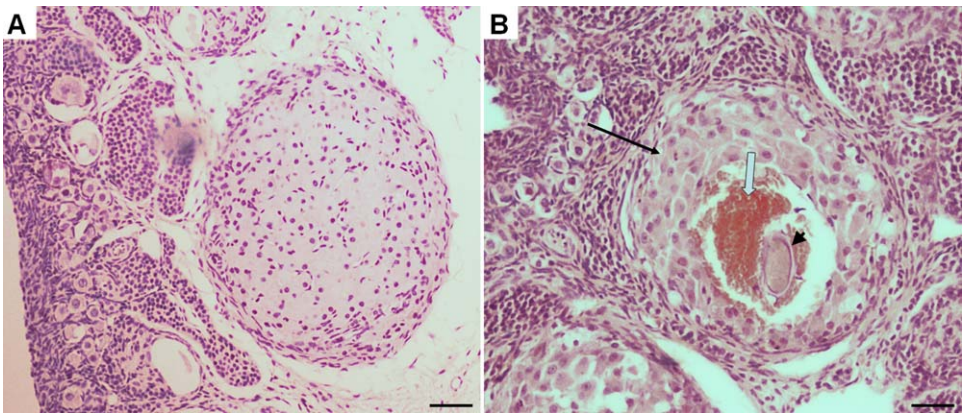

FIG. 1. Histological differentiation between primary and secondary corpora lutea at midgestation in the pregnant vizcacha ovary. Typical appearance of primary corpora lutea (**A**) showing fully luteinized cells and secondary corpora lutea (**B**), newly formed at midgestation, displaying luteinization in progress (arrow), retention of the oocyte (arrowhead), and blood remains (white arrow) in the antral cavity. Bar = 50 μm.

Tissue Collection

Animals were anesthetized by the intramuscular injection of 13.5 mg/kg body weight ketamine chlorhydrate (Holliday Scott S.A.) and 0.6 mg/kg body weight xylazine chlorhydrate (Richmond Laboratories), and blood samples were taken by cardiac puncture. After bleeding, animals were killed by trained technical staff by an intracardiac injection of 0.5 ml/kg body weight Euthanyle (sodic pentobarbital, sodic diphenilhidanthoine; Brouwer S.A.), and brains were immediately removed. Isolated brains were either fixed in cold 4% neutral-buffered paraformaldehyde (PFA; Sigma Aldrich Inc.) for immunohistochemical studies or immediately frozen in dry ice and stored at −80°C for protein analysis.

Serum Progesterone Determination

Blood samples were centrifuged for 15 min at 3000 rpm and the serum fraction aliquoted and stored at −80°C. To determine P4 serum levels, the EIAgen 17a-OH Progesterone Kit (Adaltis SRL) was used according to the manufacturer's instruction. A direct solid-phase enzyme immunoassay that detects a range of 0.18–40.0 ng/ml of P4 was developed. The absorbance of the solution measured at 450 nm (μQuant Microplate Spectrophotometer; Bio-tek Instruments Inc.) was inversely related to the concentration of P4 in the sample. Calculation of P4 content was made by reference to a calibration curve. All captured animals were evaluated in each group.

Radioimmunoassay for LH Detection

Serum LH content was determined by radioimmunoassay (RIA) with kits from the National Hormone and Pituitary Program, National Institute of Diabetes and Digestive and Kidney Diseases. Results were expressed in terms of rat LH standards, using the following standards: for LH iodination, r-LH-I10, reference preparation rat LH-RP-3 (AFP7187B) and anti-rat LH-S11 (AFPC697071P) [20]. Assay sensitivity was 0.31 ng/ml. Intra- and interassay coefficients of variation were 7.2% and 11.4%, respectively. All captured vizcachas were evaluated. A pooled pituitary homogenate of high LH content was serially diluted to confirm the parallelism with the rat standard curve (Supplemental Fig. S1; available online at www.biolreprod.org).

RIA for GnRH Detection

After rapid brain removal, whole hypothalamus was dissected out, and the anterior hypothalamus (AH) and medium-basal hypothalamus (MBH) were isolated. AH, including the preoptical area (POA), was isolated surrounded by the anterior, posterior, and lateral borders of the optic chiasm (oc). MBH, including medium-eminence (ME), was isolated surrounded by the posterior and lateral borders of the oc and the anterior border of the mammillary bodies. The in-depth limit of the fragments was the subthalamic sulcus (approximately 4-mm depth). Both fragments were frozen and stored at −80°C until used. Tissues were homogenized in 100 μl 0.1 N HCl and centrifuged for 30 min at 13 000 × *g* and supernatants recovered. All procedures were carried out at 4°C. GnRH concentration was determined as previously described [20]. Briefly, samples were analyzed in duplicate using anti-GnRH antiserum (rabbit polyclonal HU60, which recognizes mGnRH and cGnRH-II, final dilution 1:50 000) kindly provided by Dr. Urbanski (Division of Neuroscience, Oregon National Primate Research Center). GnRH was iodinated with ^{125}I (NEZ 033H Iodine 125; Perkin Elmer, Life and Analytical Science) by the chloramine-T method [21]. Intra- and interassay coefficient of variation was 7.2% and 11.6%, respectively. The detectability limit was 1.5 pg. Protein content of each sample was determined by Bradford method [22]. Results were expressed as the ratio between GnRH value obtained by RIA and the protein content. Five to six animals per group were tested.

SDS-PAGE and Western Blotting

AH and MBH fragments, including POA and ME, respectively, were homogenized (1:3 w/v) in RIPA buffer (0.1 M PBS, pH 7.4, 1% Igepal, 0.5% sodium deoxycolate, 0.1% SDS), containing 0.1 μM apotionin, 0.1 μM leupeptin, 0.1 μM pepsin, and 0.1 mM phenylmethylsulfonyl fluoride. All procedures were carried out at 4°C. Homogenates were centrifuged for 30 min at 14 000 × *g* and the supernatants collected. To confirm specificity of the antibody, a whole hypothalamus from a nonovulating female laboratory mouse, processed in the same conditions, was included as tissue control. To use similar amounts of proteins, protein concentration was determined by Bradford method [22], using bovine serum albumin as standard. Equal amounts of solubilized proteins were mixed (4:1) with sample buffer (1 M Tris-HCl, pH 6.8, 10% w/v SDS, 30% v/v glycerol, 0.1% w/v bromophenol blue, and 0.15% w/v 2-mercaptoethanol) and heated for 3 min at 100°C. Samples were separated on an SDS-polyacrylamide gel (29:1 acrylamide:bis acrylamide; Bio-Rad Laboratories), 10% running gel with 4% stacking gel, with 0.25 M Tris-glycine, pH 8.3, as the electrolyte buffer, in an electrophoresis cell (Mini-PRO-TEAN II Electrophoresis Cell; Bio-Rad Laboratories). For Western blot analysis, proteins were electrotransferred to a 0.2-mm polyvinylidene difluoride membrane (Immobilon-P; EMD Millipore Corporation) at 250 mA for 2 h. For protein identification, membranes were blocked 1 h at room temperature with 5% powder milk in PBS containing 0.1% Tween 20. Then they were incubated overnight at 4°C with anti-PR rabbit polyclonal IgG (1:1000 dilution, PR [C-19], Santa Cruz Biotechnology Inc.). This antibody detects the C-terminus of both A and B isoforms of PR, and its specificity has been well documented [23–25]. To develop immunoreactivity, membranes were incubated with goat anti-rabbit IgG-HRP (1:3000 dilution; Bio-Rad Laboratories) and ECL Plus kit (GE Healthcare Ltd) to chemiluminiscence development. To normalize the results, monoclonal IgG anti-β-actin (1:5000 dilution) (AC-15; Sigma Aldrich) was used in the same membranes and revealed out with goat anti-mouse IgG-HRP (1:3000 dilution; Bio-Rad Laboratories). Membranes were scanned with ImageQuant 350 (GE Healthcare Bio-Sciences AB) and dot-blots analyzed with Image-Pro Plus software (Image-Pro Plus 6; Media Cybernetics Inc.). The estimation of band size was performed using a prestained protein ladder (PageRuler; Fermentas UAB) as a molecular weight marker. Results were expressed as the relative optical density (ROD) of PR/ROD β-actin. Because Western blotting is a semiquantitative technique, ROD of nonovulating animals was considered as 100%, and values were expressed as the percentage of change of ovulating with respect to nonovulating animals. Four to five animals were tested per group.

Immunohistochemistry and Immunofluorescence with Confocal Microscopy

After removal, brains were coronally sectioned in blocks of 5–7 mm thick, fixed in cold 4% PFA in 0.1 M PBS (pH 7.4) for 72 h, dehydrated through a graded series of ethanol, and embedded in paraffin. For each specimen, the brain region containing the hypothalamus was entirely cut to serial coronal sections (5 μm thick) and mounted onto coated slides. Sections were dewaxed in xylene and rehydrated through a decreasing series of ethanol (100%, 95%, and 70%). One of every 10 sections was separated to perform classical hematoxylin staining to localize hypothalamic nuclei POA and ME according to previous description [15]. Adjacent sections were used for immunohistochemical assays. Antigen retrieval was performed by boiling sections in 10 mM sodium citrate buffer (pH 6) for 20 min, followed by 20 min of cooling at room temperature. Then endogenous peroxidase activity was blocked with 2% hydrogen peroxide in methanol for 30 min. After that, sections were incubated with a blocking solution containing 10% normal rabbit serum in PBS, pH 7.4, for 1 h. PR immunoreactivity was detected by incubating slides overnight at room temperature with an anti-PR rabbit polyclonal IgG (1:200 dilution; PR [C-19]; Santa Cruz Biotechnology). The specificity was corroborated in adjacent sections by omission of the primary antibody or by preabsorption of the anti-PR antibody with PR blocking peptide (10 μg, 1:20 dilution; PR [C-19]; Santa Cruz Biotechnology) incubated overnight in a rotator at room temperature, then followed by centrifugation for 20 min at 15 000 × *g*. Immunoreactivity was revealed with biotinylated goat anti-rabbit IgG followed by incubation with avidin-biotin complex (ABC Vectastain Elite kit; Vector Laboratories). The reaction was visualized with 3,3′ diaminobenzidine (DAB) and intensified with nickel ammonium sulfate (DAB kit; Vector Laboratories) that yields a black product. Finally, treated sections were dehydrated through a graded series of ethanol (70%, 95%, and 100%), cleared in Neo-Clear (Merck KgaA) and coverslipped. For colocalization studies, anti-PR rabbit polyclonal IgG (1:200 dilution) (PR [C-19]; Santa Cruz Biotechnology) and anti-GnRH mouse monoclonal IgG (1:200 dilution; EMD Millipore Corporation) were employed. To corroborate anti-GnRH antibody specificity, which has already been reported [15, 26, 27], adjacent sections were incubated by omission of the primary antibody or by preabsorption of the anti-GnRH antibody with LHRH synthetic peptide (10 μg, 1:20 dilution; L7134; Sigma) incubated overnight in a rotator at room temperature followed by centrifugation for 20 min at 15 000 × *g*. Following overnight incubation with both primary antibodies, colocalization studies were performed by immunofluorescence technique using FITC-coupled donkey anti-mouse IgG (Vector Laboratories) and Alexa-Fluor 555 coupled donkey anti-rabbit IgG (Invitrogen Corp.), both at a 1:250 dilution. To corroborate anti-PR and anti-GnRH antibodies specificity, adjacent sections were incubated by preabsorption of the anti-PR antibody with PR blocking peptide or preabsorption of the anti-GnRH antibody with LHRH synthetic peptide as described above for immunohistochemistry. Five to six animals were tested per group.

Image Analysis

Before assays, care was taken in selecting anatomically matching areas among animals for each analyzed hypothalamic nucleus. Six sections for each animal were analyzed. Microscope images of PR immunoreactivity were captured with an optic microscope (BX40; Olympus Optical Corporation), fitted with a digital camera (390CU 3.2-megapixel CCD camera; Micrometrics) and analyzed using Image-Pro Plus software (Image-Pro Plus 6, Media Cybernetics). All images were taken the same day under the same light to avoid external variations. For immunoreactive area (IA) measurement, four distinct areas were chosen based on their anatomical involvement in GnRH synthesis and secretion. These areas included mPOA, ventromedial nucleus (VMN) of the hypothalamus, SON, and ME. To eliminate nonspecifically stained cells, only those cells that had a gray level darker than a defined ''threshold'' criterion (defined as the optic density three times higher than the mean background density) were considered. The mean background density was measured in a region devoid of PR immunoreactivity, immediately adjacent to the analyzed region. IA was determined by measuring the area covered by ''thresholded'' pixels (pixels with a gray level higher than the defined ''threshold'' density). The gray level of threshold setting was maintained for all studied animals. Particles smaller than a pre-established number of pixels were excluded. The percentage of PR stained area from the total analyzed area was considered. Colocalization of PR and GnRH was studied by immunofluorescence using a Nikon C1 Plus Laser microscope (Nikon Inverted Research Microscope Eclipse Ti; Nikon Corp.), and images were analyzed with the EZ-C1 software, version 3.9 (Nikon Ltd). Adobe Photoshop CS5 software (Adobe Systems Inc.) was used for digital manipulation of brightness and contrast when preparing the shown images.

Statistical Analysis

Values are expressed as mean ± SD. Each experiment was performed in duplicate. Results were evaluated using one-way analysis of variance, and comparisons among groups were made by Fisher, Scheffé, and Bonferroni multiple comparison tests. Statistical analysis was performed using Prism 4.0 (GraphPad Software Inc.). Differences were considered significant when $P < 0.05$.

RESULTS

Progesterone and Luteinizing Hormone Levels at Different Reproductive Stages

P4 and LH serum measurements showed some striking differences among the evaluated groups (Fig. 2). Ovulating females showed a marked 10-fold increase in P4 serum levels compared with nonovulating females (6.56 ± 1.43 ng/ml and 0.55 ± 0.03 ng/ml, respectively). Midpregnant females also showed significantly increased serum P4, three times higher compared with early-pregnant animals (12.33 ± 1.12 ng/ml and 3.75 ± 1.02 ng/ml, respectively; Fig. 2A). Serum LH showed circulating levels close to null in nonovulating females that rose up as females went through ovulation (0.41 ± 0.33 ng/ml and 2.88 ± 0.97 ng/ml, respectively; Fig. 2B). Midpregnant females also showed significantly increased values of serum LH with respect to early-pregnant animals (0.47 ± 0.35 ng/ml and 3.47 ± 1.09 ng/ml, respectively; Fig. 2B).

GnRH Expression Throughout the Different Reproductive Stages

Variations in the levels of hypothalamic GnRH were observed among the different reproductive stages and between both hypothalamic regions, AH and MBH, as well. Ovulating females showed a significant reduction in GnRH content with respect to nonovulating animals, and such decrement was observed in both regions (70% in AH and 75% in MBH; Fig. 3, A and B). During pregnancy, midpregnant females exhibited a significant increase in GnRH content in relation to early-pregnant animals, with a higher increase at MBH (2.5-fold) than AH (0.6-fold; Fig. 3, A and B). Both ovulating and nonovulating females showed a similar GnRH/total proteins ratio in AH and MBH (Fig. 3C). However, GnRH content distribution was biased in the hypothalamus of ovulating pregnant females, with a lower content in AH than MBH (Fig. 3C).

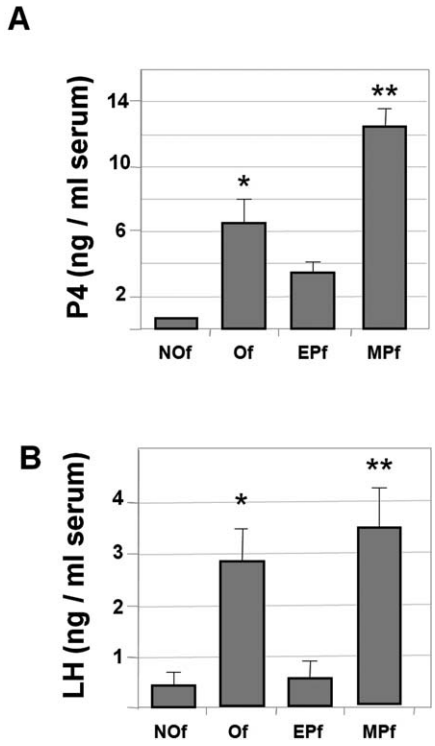

FIG. 2. Progesterone and LH serum levels in pregnant and nonpregnant *L. maximus* females. A significant increment of P4 serum levels (**A**) and LH serum levels (**B**) were observed in ovulating females (Of) versus nonovulating nonpregnant females (NOf; $*P < 0.05$) as well as in midpregnant females (MPf) versus early-pregnant animals (EPf; $**P < 0.05$). n = 15–20 animals per group.

Progesterone Receptor Expression Throughout Gestation

Only PRB isoform (116 kDa) was detected by Western blot, with no significant variations in AH and MBH (Fig. 4A) in nonovulating females. A comparable level of PRB expression was detected in control mouse hypothalamus (Fig. 4A). At ovulation, a comparable increase in PRB was detected in AH both in nonpregnant and pregnant females (Fig. 4B). A 37% increment was detected in ovulating females with respect to nonovulating animals, whereas midpregnant vizcachas showed a 32% increment compared with early-pregnant females (Fig. 4B). On the other hand, PRB expression in MBH was not altered in nonpregnant animals regardless of ovulation (Fig. 4C). Nevertheless, midpregnant vizcachas showed a significant 38% increase in PRB expression compared with early-pregnant females (Fig. 4C).

Localization of Progesterone Receptors in the Hypothalamus of the Vizcacha

At the most rostral region of the POA (Fig. 5A), PR immunoreactive neurons were found in the vertical portion of the diagonal band of Brocca (DBB; Fig. 5C) with a cytoplasmic vesicular distribution pattern (Fig. 5C, inset). At the medial POA (mPOA) (Fig. 5B), PR-expressing cells were localized around the third ventricle (IIIV) below the anterior

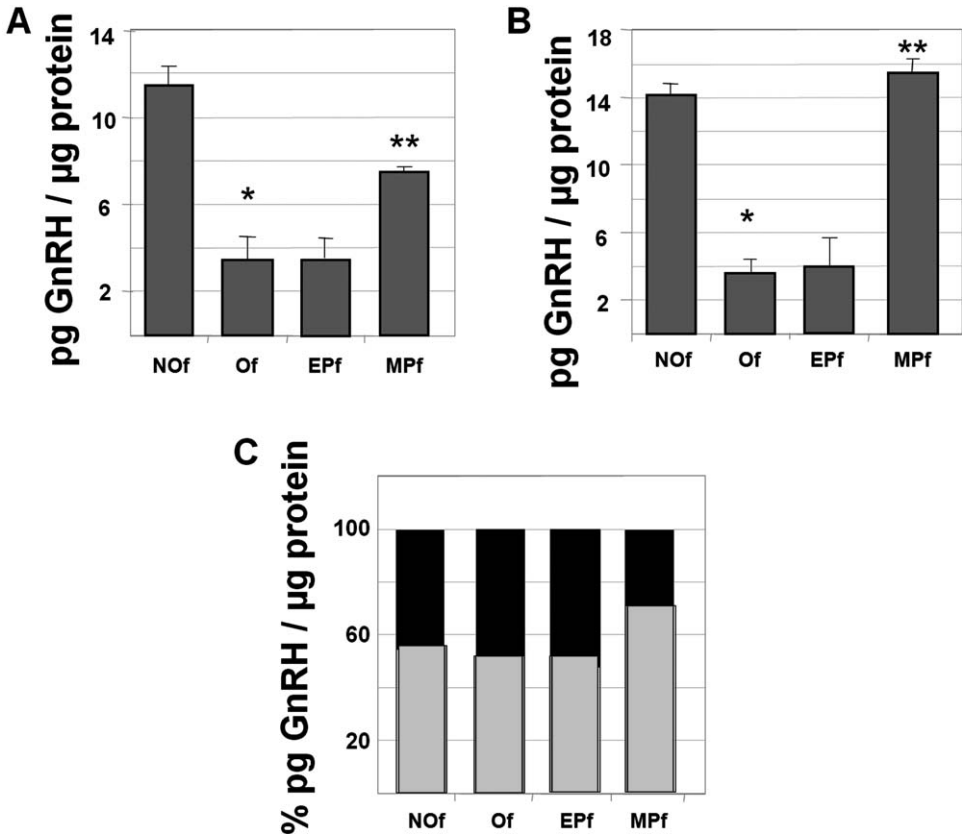

FIG. 3. GnRH content in the hypothalamus of *L. maximus* throughout the reproductive cycle. A similar pattern of circulating GnRH was found both in the AH (**A**) and in the MBH (**B**). Ovulating females (Of) showed a significant decrease in GnRH compared with nonovulating nonpregnant females (NOf; $*P < 0.05$), whereas midpregnant females (MPf) presented a significant increment versus early-pregnant animals (EPf; $**P < 0.05$). **C**) GnRH content distributed in a balanced way between the AH (black bars) and MBH (gray bars), except in MPf, which showed a lesser content of GnRH in the AH. n = 5–6 animals per group.

commissure (ac; Fig. 5D), in neurons of mPOA with both nuclear or cytoplasmic distribution (Fig. 5E, upper inset), in the cytoplasm of bipolar neurons at the lateral POA (lPOA; Fig. 5E, lower inset), in neurons around the lower IIIV (Fig. 5F), in neurons of the suprachiasmatic nucleus (SCN; Fig. 5F), and in the ventrolateral POA, where the SON resides (Fig. 5G) exclusively with cytoplasmic localization (Fig. 5G, inset). The intensity of the DAB reaction product varied among areas, neurons from mPOA, lPOA, and DBB being the most densely stained. In ME (Fig. 6A), PR immunoreactive neurons were found scattered throughout the VMN (Fig. 6B) with cytoplasmic localization (Fig. 6C) and only a few immunoreactive neurons localized in arcuate nucleus (Arc) and ME regions (Fig. 6D). A dense population of intense PR immunopositive cells was extended into the infundibular region (Fig. 6D). All studied groups exhibited PR-immunoreactive cells distributed in the same areas of the POA; however, differences in the immunoreactive area were observed when morphometric studies were developed. Medial POA and SON (Figs. 6, A–D, and 8, A and B) of ovulating and midpregnant animals showed increased PR immunoreactive area with respect to nonovulating animals. A marked significant increment in the mPOA and SON of midpregnant females with respect to early-pregnant vizcachas was observed (Figs. 7, A–D, and 8, A and B). In the VMN, PR immunoreactive area was also significantly increased in ovulating animals with respect to nonovulating vizcachas (Figs. 7, E and F, and 8C). In the ME, only a few PR immunoreactive cells were found in almost all animals. Surprisingly, the midpregnant group showed a significantly increased PR immunoreactive area (a 3.8-fold increment) with respect to early-pregnant vizcachas (Figs. 7, G and H, and 8D). No PR-specific labeling was detected after preabsorption of the primary antibody with PR peptide in adjacent sections or after omission of PR primary antibody (not shown).

Progesterone Receptors and GnRH Colocalization in the Hypothalamus of the Plains Vizcacha

GnRH immunoreactivity was detected in neurons scattered throughout mPOA (Fig. 9A) and SON (Fig. 9D). GnRH immunoreactivity was detected with a granular pattern in the cytoplasm of neurons and distributed in beads in varicosities of hypothalamic dendrites (Fig. 9A). In addition, a homogeneous GnRH immunoreactive pattern was found in the cytoplasm of neurons in the SON (Fig. 9D). The pattern of GnRH immunostaining was similar in all evaluated groups. In the mPOA, a few GnRH immunoreactive neurons were found within many PR immunoreactive neurons (Fig. 9B). Only a few cells showed coexpression of both proteins (Fig. 9C), while PR exclusively immunoreactive cells were localized adjacent to GnRH immunopositive cells (Fig. 9C). In addition, all neurons of the SON showed PR immunoreactivity (Fig. 9E), and most of them presented colocalization of PR and GnRH (Fig. 9F). An almost identical immunoreactive pattern was observed in all analyzed groups. No GnRH-specific labeling was detected after preabsorption of the primary antibody with

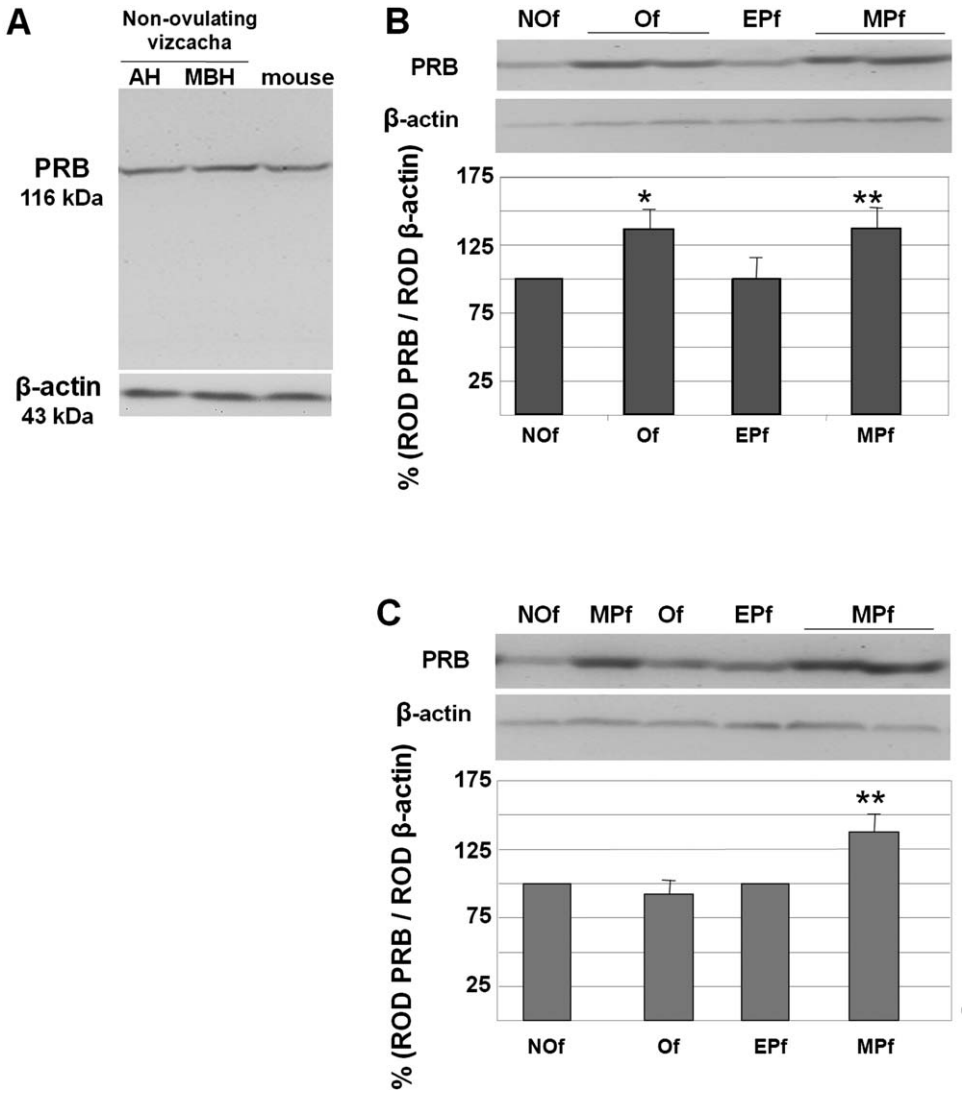

FIG. 4. Western blot analysis of PR expression in the hypothalamus of *L. maximus* throughout the different reproductive stages. A similar level of PRB (116 kDa) expression was observed in the AH and in the MBH of nonovulating nonpregnant females (NOf), comparable to mouse hypothalamus used as control tissue (**A**). In the AH, PRB expression significantly increased in ovulating females (Of) and midpregnant females (MPf; **B**). In the MBH, no differences in PRB expression were detected between NOf and Of; however, a significant increase was detected in MPf compared with early-pregnant females (EPf; **C**). Bar graphs in **B** and **C** represent PRB ROD expressed as percentage of β-actin loading control. Data are plotted as mean ± SD. *Statistically significant differences between NOf and Of, $P < 0.05$; **statistically significant differences between EPf and MPf, $P < 0.05$. n = 5–6 animals per group.

GnRH synthetic peptide in adjacent sections or after omission of GnRH primary antibody (not shown).

The ME showed GnRH immunoreactive beaded fibers radially orientated with respect to the recessus mammillaris of the IIIV and around vessels of the primary plexus of the hypothalamic-hypophyseal portal vessels (Fig. 10, A and C). A similar GnRH distribution was observed in all evaluated groups. The ME of nonpregnant and early-pregnant animals did not show PR immunoreactivity or showed just a few cells with a faint PR expression (Fig. 10, A and B). However, ME of midpregnant females showed PR expression in the cytoplasm of cells adjacent to GnRH immunoreactive fibers all along their extension (Fig. 10, C and D).

DISCUSSION

The results presented above show that the South American plains vizcacha has an active hypothalamic-hypophyseal (H-H) axis during gestation and an active ovary that progresses to preovulatory follicular formation and contributes luteinized unruptured follicles at midgestation. This correlation suggests a possible role of the H-H axis in the modulation of preovulatory follicular formation and addition of luteinizing unruptured follicles at midgestation in *L. maximus*.

The ovulating vizcachas had significantly increased levels of serum P4 and LH compared with nonovulating animals regardless of the pregnancy state. P4 levels in midpregnant females were comparable to previous results [12]. It is worth noticing that the addition of luteinizing unruptured follicles at midpregnancy was accompanied by a considerable increase in P4 and LH levels with respect to early pregnancy. Although those hormonal levels may decrease GnRH expression in the nonpregnant vizcacha, they do not seem to suppress GnRH expression in the midpregnant female, allowing the H-H-G axis activity during pregnancy. Taking into account the high percentage of luteinization of unruptured follicles observed at midgestation, the existence of a light P4-negative feedback

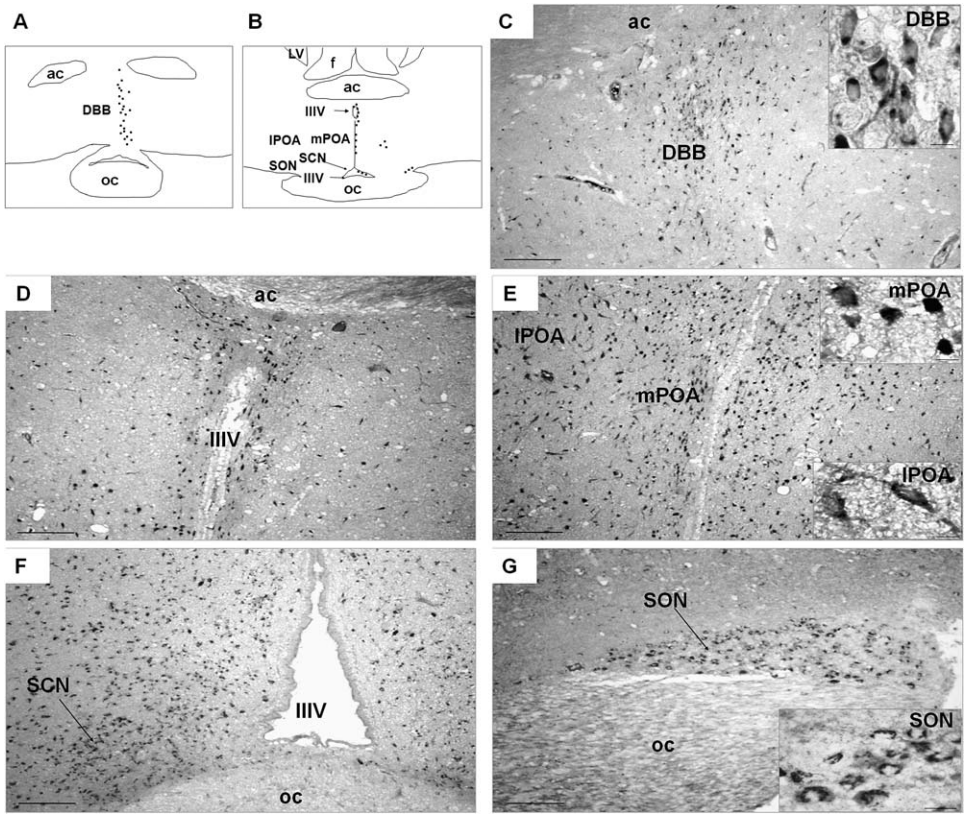

FIG. 5. Immunolocalization of PR in the POA of the hypothalamus of the vizcacha. Schematic representations of most rostral (**A**) and mPOA (**B**) of the hypothalamus, with PR distribution indicated as black spots. PR immunolocalizes in the DBB (**C**), around the IIIV (**D**), in the lPOA and mPOA (**E**), in the SCN (**F**), and in the SON (**G**). **D** and insets in **C** and **E**) Details of cytoplasmic or nuclear PR distribution. Representative images shown in **C**–**E** correspond to a nonovulating nonpregnant female, while images shown in **F** and **G** correspond to a midpregnant female. ac, anterior commissure; f, formix; inf, infundibulus; LV, lateral ventricle; oc, optic chiasm. Bars = 100 μm (**C**–**F**), 130 μm (**G**), 10 μm (insets in **C** and **E**), and 20 μm (inset in **G**).

over LH and GnRH cannot be discarded. Nevertheless, if negative feedback exists, it seems to be permissive to induce luteinization of unruptured preovulatory follicles. On the other hand, the presence of secondary corpora lutea in ovulating females as found in midpregnant females, suggests that luteinization of unruptured follicles might result from an insufficient secretion of LH since the increase in LH at ovulation and midgestation is comparable.

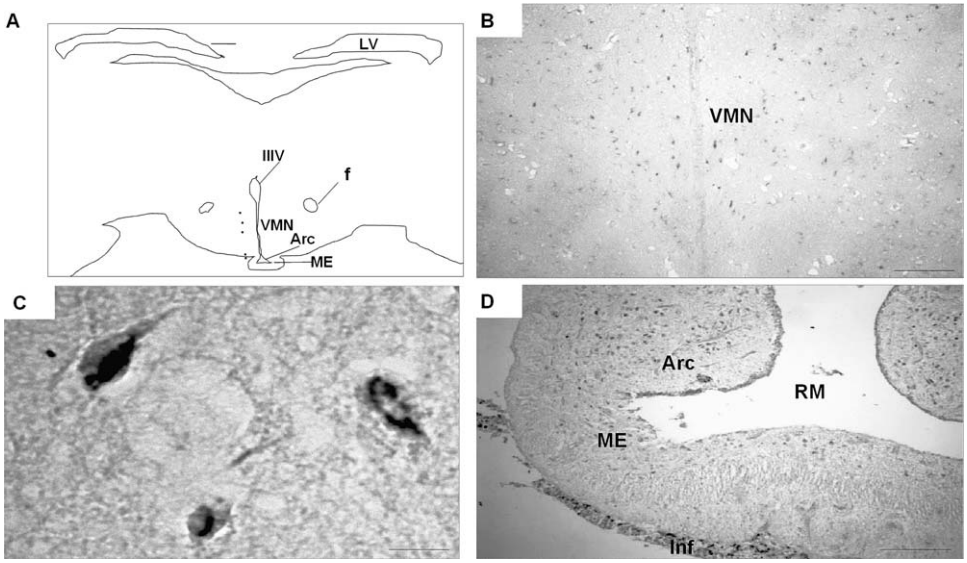

FIG. 6. Immunolocalization of PR in the ME of the hypothalamus of vizcacha. Schematic representation of the ME level of the hypothalamus of vizcacha with PR distribution (shown as spots; **A**). Representative images of a nonovulating nonpregnant vizcacha with PR immunolocalization in the VMN (**B**), Arc (**D**), and ME (**D**) are shown. Cellular distribution of PR at VMN is shown in **C**. IIIV, third ventricle; f, fornix; inf, infundibulus; LV, lateral ventricle; RM, recessus mammillaris. Bars = 100 μm (**B**), 10 μm (**C**), and 160 μm (**D**).

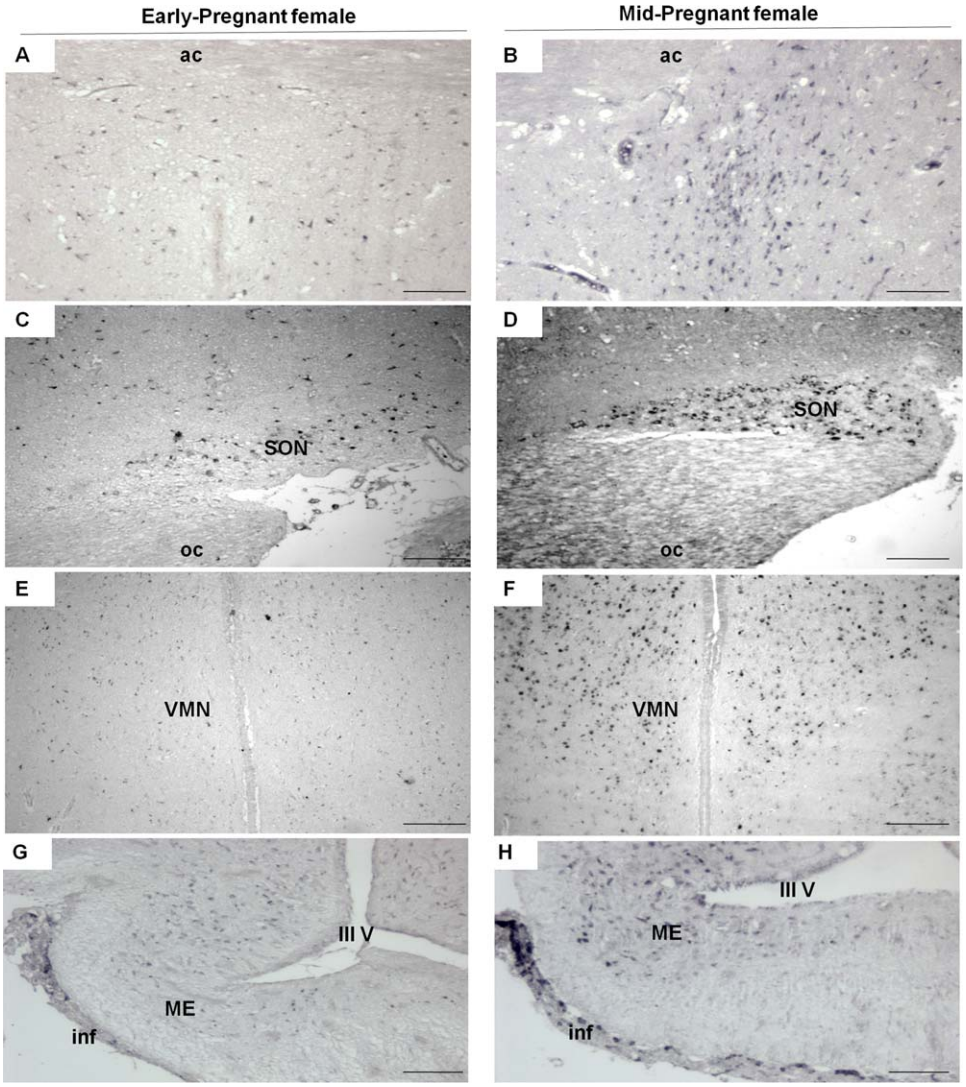

FIG. 7. Differences in PR expression between early-pregnant and midpregnant vizcachas. Representative images of PR immunolocalization in early (**A**, **C**, **E**, and **G**) and midpregnant vizcacha (**B**, **D**, **F**, and **H**). PR immunoreactivity is shown around the IIIV below the ac (**A** and **B**), in the SON (**C** and **D**), in the VMN (**E** and **F**), and in the ME (**G** and **H**). inf, infundibulus; oc, optic chiasm. Bars = 100 μm (**A**, **B**, **E**, and **F**), 130 μm (**C** and **D**), 250 μm (**G**), and 160 μm (**H**).

The increment at hypothalamic GnRH and hypophyseal LH during gestation, which correlates with the presence of secondary corpora lutea [12], may suggest a link between H-H axis and ovaries; however, it cannot be discarded that the hypothalamic GnRH increase during gestation would point out an inhibition in the neuropeptide delivery with a consequent local increment. Future approaches focusing on the study of cellular mechanisms would help us understand if H-H-G axis activity is maintained during pregnancy. In addition, the possible action of placenta or fetus on the increasing ovarian progesterone secretion, influencing the H-H axis during pregnancy, should not be discarded.

Considering that most areas responsible for GnRH synthesis reside at the AH region while MBH containing ME is involved mostly in GnRH delivery, the observed changes in GnRH distribution between AH and MBH in midpregnant animals could indicate changes in its ratio of synthesis/secretion during different reproductive stages. On the other hand, the high levels of P4 detected in midpregnant females were not able to induce negative feedback on PR expression. Significant increased levels of PR were observed in the groups with high levels of serum P4, and this correlation occurred in both AH and MBH. Midpregnant and ovulating vizcachas showed higher levels of PR content than nonovulating females. This constitutes also a key point for future studies to elucidate the mechanisms of P4 inhibition of negative feedback during gestation.

The relative distribution of PR in the hypothalamus of the vizcacha is consistent with that previously described in other mammalian species, such as rat [28], mouse [29], guinea pig [30], primate [31], mink [32], cat [33], and ewe [34–36]. PR distribution was found in neurons of the POA (DBB, periventricular nucleus, mPOA, lPOA, PVN, and SCN), VMN, Arc, and ME hypothalamic areas. Surprisingly, PR immunolocalization was also observed in neurons of SON, and this detection is in agreement with a previous report in the monkey brain [37]. In addition, PR immunoreactivity in vizcacha is observed at both nuclear and cytoplasmic compartments, depending on the hypothalamic area, where a vesicular cytoplasmic distribution pattern was detected, establishing a striking difference from previous observations in other mammals that show predominant nuclear localization [37]. Genomic effects of P4 are mediated through its binding to

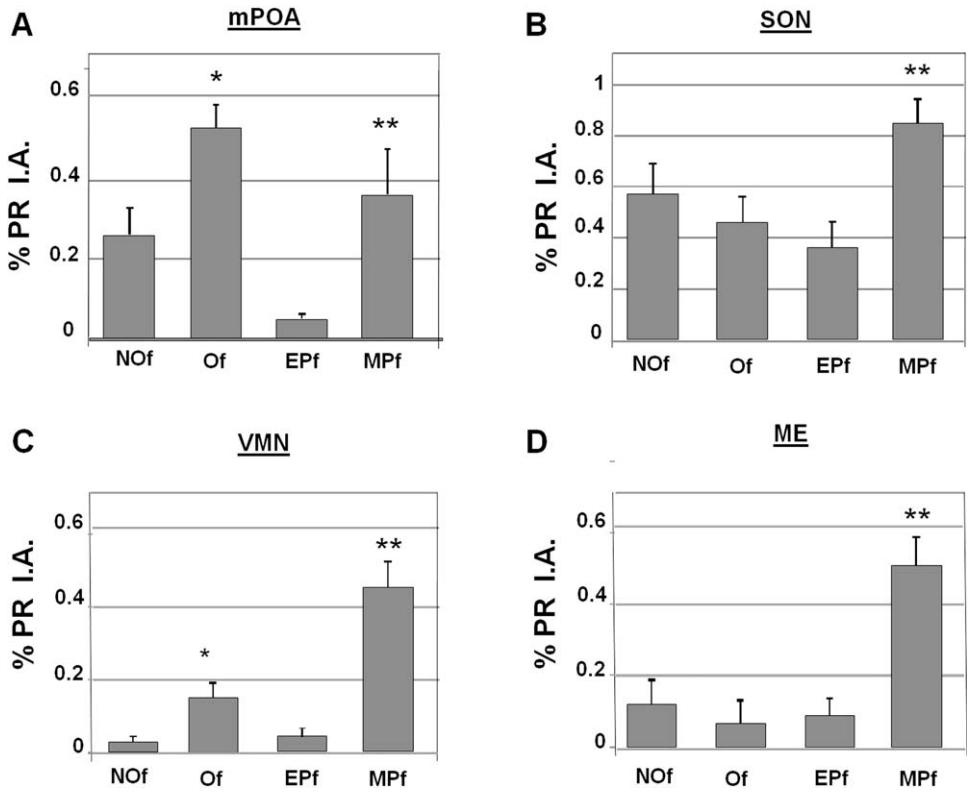

FIG. 8. Differences in PR immunoreactive area throughout different reproductive stages in *L. maximus* females. Increased PR immunoreactive area (I.A.) was observed in ovulating females (Of) with respect to nonovulating nonpregnant females (NOf) and in midpregnant females (MPf) in relation to early-pregnant females (EPf) at mPOA (**A**), SON (**B**), VMN (**C**), and ME (**D**). Graphics represent the mean ± SD. *Statistically significant differences respect to nonovulating animals ($P < 0.05$); **statistically significant differences respect to early-pregnant females ($P < 0.05$). n = 5–6 per animals group.

nuclear receptors that function as ligand-dependent transcription factors after phosphorylation. This is assumed to be the primary pathway for P4 action in the brain. However, nongenomic actions of PR have been recently described [38]. Cytoplasmic second messenger signaling cascades involving extranuclear PR that interacts with Src kinase via MAPK action can increase the phosphorylation of coactivators that act as transcription factors [39, 40]. This rapid, nonclassical progesterone action may converge with classical PR-mediated response to serve as an amplification mechanism to regulate nuclear PR action on gene transcription and translation that facilitate female reproductive behavior [38]. Both classical genomic and nonclassical nongenomic actions may be involved in the vizcacha. On the other hand, when immunohistochemistry results were compared among groups, a concordant correlation was observed between the morphometric study of immunoreactive area in all evaluated regions and the pattern of PR content detected by Western blot.

A central aim of the present work was to investigate the expression of PR in the hypothalamus of vizcacha and its relation with GnRH synthesis and secretion. Previously, we localized GnRH immunoreactivity in perikarya and processes of the vizcacha hypothalamus, including the SON [15]. GnRH is synthesized by a discrete specialized group of neurons scattered throughout the POA of the basal forebrain [41–43]. A portion of them project their axons caudally along the ventral surface of the diencephalon toward the ME, with SON as the lateral boundary. At ME, axons surround the primary plexus of the hypothalamic-hypophyseal portal vessels and release GnRH toward the anterior pituitary gland to modulate ovulation [44]. Here, we show the coexistence of PR with GnRH in neurons of mPOA and SON by confocal microscopy, suggesting a possible action of PR on GnRH neurons. In addition, the possible influence of PR on GnRH delivery was evident in midpregnant females, the only group with abundant PR cells localized along GnRH axons of the ME area. Other animals, such as mink [32], hens [45], and ewe [46], show GnRH neurons adjacently localized to PR-immunopositive neurons, but they never show both proteins in the same cell [32, 45, 46]. However, the guinea pig, which belongs to the same suborder as vizcacha and is a close evolutionary relative [13, 47], with a true luteal phase, shows a small subpopulation of GnRH neurons containing PR [48] but with an exclusive nuclear localization. We propose that in the vizcacha, just a few PR-expressing neurons may be involved in the GnRH pulse generation at mPOA; however, almost all neurons of SON may be involved in regulation of H-H-G axis function. In concordance with previous description in monkeys by Bethea et al. [37], neurons in the SON of *L. maximus* continuously express PR in spite of sustained high P4 serum levels. The lack of P4 negative feedback in these cells suggests no steroid regulation on PR expression, enabling them to continue with GnRH synthesis. Reinforcing this idea, in the early 1990s, O'Malley and colleagues [49, 50] showed that agents like 8-bromo-cyclic adenosine monophosphate (8-Br cAMP), a stimulator of cAMP-dependent protein kinase, may act on PR phosphorylation and enable PR to act as a transcription factor. This raises the possibility that PR in the vizcacha brain were functional independently of ovarian P4. Further studies to identify constitutive versus inducible PR could help to elucidate this possibility.

The present work described the hypothalamic colocalization of PR and GnRH; however, the specific variant of GnRH detected here is not known. According to its amino acid

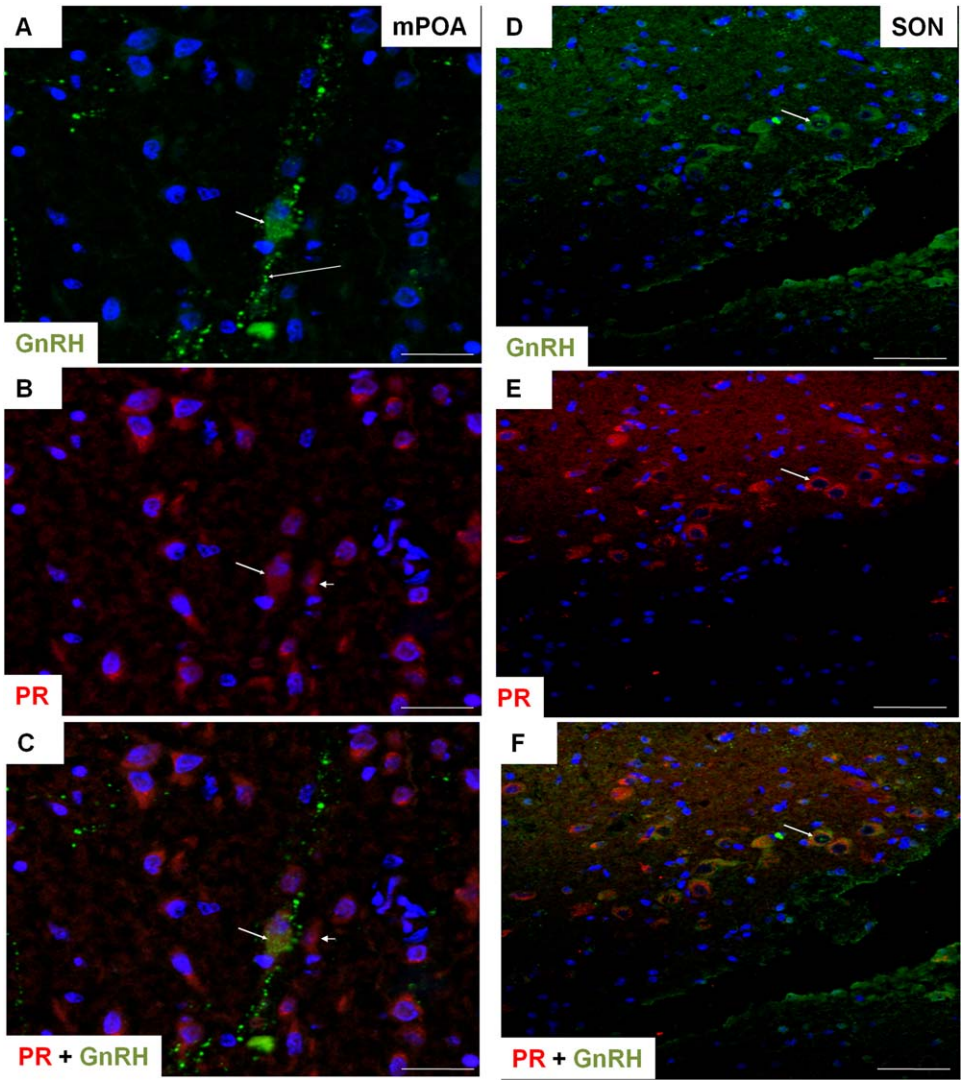

FIG. 9. Colocalization of GnRH and PR in the POA of the vizcacha hypothalamus. Representative images of GnRH and PR localization in the POA of a nonovulating nonpregnant vizcacha. GnRH was immunolocalized in the cytoplasm (arrow) and varicosities (large arrow) of neurons located in the mPOA (**A**) and SON (**D**). Colocalization of GnRH and PR was observed in cells of mPOA (**A**–**C**) and SON (**D**–**F**). Nuclei were counterstained with DAPI (blue). Green: GnRH; red: PR; green/yellow: GnRH + PR. Arrows: cytoplasmic GnRH and cytoplasmic PR; large arrow: GnRH immunoreactive varicosities; head arrow: PR immunoreactive neurons without GnRH immunoreactivity. Bars = 20 μm (**A**–**C**) and 30 μm (**D**–**F**).

sequence composition, function, localization, and embryonic origin, 24 GnRH peptides have been identified from the nervous tissue of vertebrates and invertebrates [51–54]. The first identified form of GnRH (mammalian, mGnRH, or GnRH-I) was isolated from porcine and ovine brains [55]. Later, two other variants were shown to be expressed in chicken brain (cGnRH-I and cGnRH-II) [56, 57]. A third form was described in guinea pigs (gpGnRH) [58], whereas fish harbor the highest diversity of isoforms with eight well-described variants [59]. The antibody used in this study identifies the -NH2 group at position 10, a region shared by both mGnRH and gpGnRH. Taking into account that the vizcacha is evolutionary closely related to guinea pig [9, 10, 13], it is likely that the immunolocalization of GnRH reported here encompasses both variants. On the other hand, a study on the regulation of mGnRH and cGnRH-II by P4 in a human cerebellar medulloblastoma TE671 cell line showed that mRNA of mGnRH is upregulated by P4, whereas no significant effects were observed in the mRNA expression level of cGnRH-II when cells were treated with P4 [60]. This suggests that changes at GnRH observed here may correspond to mGnRH and/or gpGnRH.

Most mammalian females show a high reduction of germinal mass from fetal life to puberty that occurs through apoptosis-dependent follicular atresia [61]. In contrast, the plains vizcacha represents an exception to massive intraovarian germ cell elimination since it shows a strong suppression of follicular apoptosis [11, 12, 14] and natural polyovulation reaching up to 800 oocytes per reproductive cycle [9]. It is worth mentioning that the elevated expression of GnRH and PR in the hypothalamus of this rodent, despite the level of P4, is correlated with a high level of ovarian activity and the presence of preovulatory follicles at midgestation. Whether this is an indication of a special modulation of the H-H-G axis that enables ovulation at midgestation and how this can relate to the increased follicular population arising from the absence of apoptosis-dependent follicular atresia deserves to be investigated. The polyovulatory phenotype in *L. maximus* has been regarded as an alternative way to apoptosis-dependent atresia in massive germ cell elimination; it is tempting to suppose that

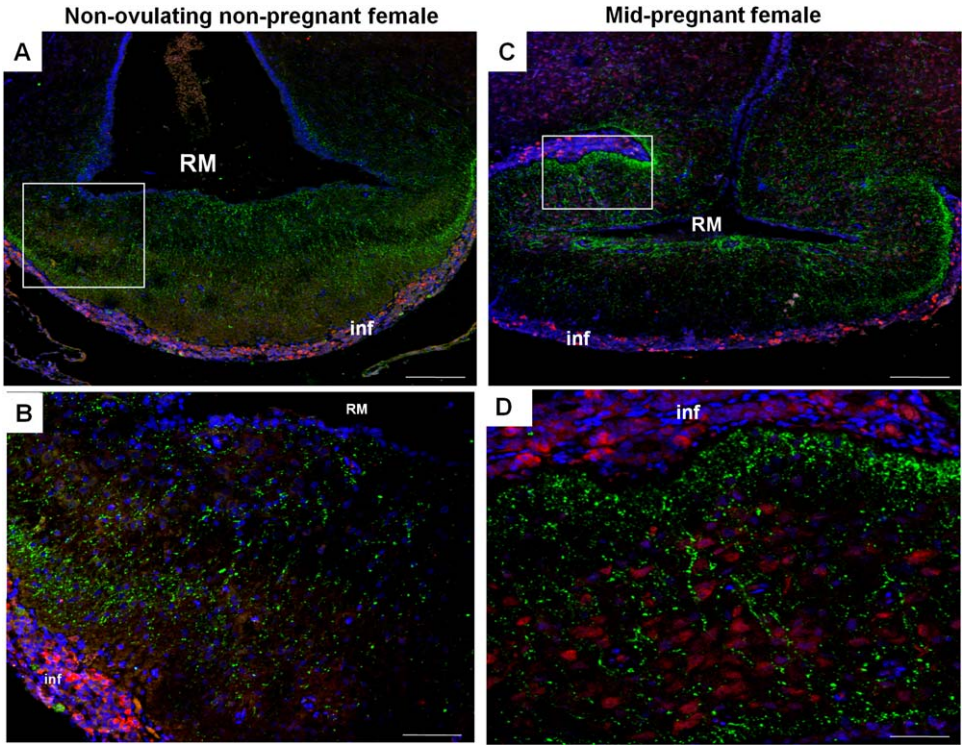

FIG. 10. Localization of GnRH and PR in the ME of the vizcacha hypothalamus. Representative images of GnRH and PR localization in the ME of a nonovulating nonpregnant female (**A** and **B**) and a midpregnant vizcacha (**C** and **D**). **B** and **D** are zoom images of the squares drawn in **A** and **C**, respectively. Only midpregnant animals showed PR immunoreactivity in cells adjacently localized to GnRH immunoreactive dendrites (**D**). Nuclei were counterstained with DAPI (blue). Green: GnRH; red: PR. inf, infundibulus; RM, recessus mammillaris. Bar = 100 μm (**A** and **C**), 25 μm (**B**), and 20 μm (**D**).

a possible activity of the H-H-G axis during gestation may support this kind of elimination even during pregnancy.

ACKNOWLEDGMENT

The authors are especially grateful to the personnel of ECAS for their invaluable help in trapping and handling the animals, to Dr. Sergio Ferraris and his veterinarian staff for their essential help on vizcachas handling and anesthetizing, to Ms. María Grisel Clausi Schettini for her excellent technical assistance in tissue processing, and to Mr. Roberto Fernández for his technical assistance in confocal microscopy.

REFERENCES

1. McKenna NJ, Lanz RB, O'Malley BW. Nuclear receptor co-regulators: cellular and molecular biology. Endocr Rev 1999; 20:321–344.
2. Micevych P, Sinchak K. Synthesis and function of hypothalamic neuroprogesterone in reproduction. Endocrinology 2008; 149:2739–2742.
3. Goodman RL, Karsch FJ. Pulsatile secretion of luteinizing hormone: differential suppression by ovarian steroids. Endocrinology 1980; 107: 1286–1290.
4. Skinner DC, Evans NP, Delaleu B, Goodman RL, Bouchard P, Caraty A. The negative feedback actions of progesterone on gonadotropin-releasing hormone secretion are transduced by the classical progesterone receptor. Proc Natl Acad Sci U S A 1998; 95:10978–10983.
5. Thackray VG, Hunnicutt JL, Memon AK, Ghochani Y, Mellon PL. Progesterone inhibits basal and gonadotropin-releasing hormone induction of luteinizing hormone beta-subunit gene expression. Endocrinology 2009; 150:2395–2403.
6. Solomon S. Formation and metabolism of neutral steroids in the human placenta and fetus. J Clin Endocrinol Metab 1966; 26:762–772.
7. Clarke CL, Sutherland RL. Progestin regulation of cellular proliferation. Endocr Rev 1990; 11:266–301.
8. Lydon JP, DeMayo FJ, Funk CR, Mani SK, Hughes AR, Montgomery CA Jr, Shyamala G, Conneely OM, O'Malley BW. Mice lacking progesterone receptor exhibit pleiotropic reproductive abnormalities. Gene Dev 1995; 9: 2266–2278.
9. Weir BJ. The reproductive physiology of the plains viscacha, *Lagostomus maximus*. J Reprod Fertil 1971; 25:355–363.
10. Weir BJ. The reproductive organs of the female plains viscacha, *Lagostomus maximus*. J Reprod Fertil 1971; 25:365–373.
11. Jensen F, Willis MA, Albamonte MS, Espinosa MB, Vitullo AD. Naturally suppressed apoptosis prevents follicular atresia and oocyte reserve decline in the adult ovary of *Lagostomus maximus* (Rodentia, Caviomorpha). Reproduction 2006; 132:301–308.
12. Jensen F, Willis MA, Leopardo NP, Espinosa MB, Vitullo AD. The ovary of the gestating South American plains vizcacha (*Lagostomus maximus*): suppressed apoptosis and corpora lutea persistence. Biol Reprod 2008; 79: 240–246.
13. Jackson JE, Branch LC, Villarreal D. Lagostomus maximus. Mamm Species 1996; 543:1–6.
14. Leopardo NP, Jensen F, Willis MA, Espinosa MB, Vitullo AD. The developing ovary of the South American plains vizcacha, *Lagostomus maximus* (Mammalia, Rodentia): massive proliferation with no sign of apoptosis-mediated germ cell attrition. Reproduction 2011; 141:633–641.
15. Dorfman VB, Fraunhoffer N, Inserra PIF, Loidl CF, Vitullo AD. Histological characterization of gonadotropin-releasing hormone (GnRH) in the hypothalamus of the South American plains vizcacha (*Lagostomus maximus*). J Mol Histol 2011; 42:311–321.
16. Kineman RD, Leshin LS, Crim JW, Rampacek GB, Kraeling RR. Localization of luteinizing hormone-releasing hormone in the forebrain of the pig. Biol Reprod 1988; 39:665–672.
17. Jackson JE. Determinación de edad en la vizcacha (*Lagostomus maximus*) en base al peso del cristalino. Vida Silv 1986; 1:41–44.
18. Health Research Extension Act of 1985, Public Law 99–158. Animals in Research. 20 November 20 1985.
19. Llanos AC, Crespo JA. Ecología de la vizcacha (*Lagostomus maximus maximus* Blainv.) en el nordeste de la Provincia de Entre Ríos. Rev Invest Agric 1952; 6:289–378.
20. Catalano PN, Di Giorgio N, Bonaventura MM, Bettler B, Libertun C, Lux-Lantos VA. Lack of functional GABA(B) receptors alters GnRH physiology and sexual dimorphic expression of GnRH and GAD-67 in the brain. Am J Physiol Endocrinol Metab 2010; 298:E683–E696.
21. Greenwood FC, Hunter WM, Glover JS. The preparation of ^{131}I-labelled human growth hormone of high specific radioactivity. Biochem J 1963; 89:114–123.

22. Bradford MM. Rapid and sensitive method for the quantitation of microgram quantities of protein utilizing the principle of protein-dye binding. Anal Biochem 1976; 72:248–254.
23. Amazit L, Roseau A, Khan JA, Chauchereau A, Tyagi RK, Loosfelt H, Leclerc P, Lombès M, Guiochon-Mantel A. Ligand-dependent degradation of SRC-1 is pivotal for progesterone receptor transcriptional activity. Mol Endocrinol 2011; 25:394–408.
24. Raman V, Tamori A, Vali M, Zeller K, Korz D, Sukumar S. HOXA5 regulates expression of the progesterone receptor. J Biol Chem 2000; 275: 26551–26555.
25. Wargon V, Fernandez SV, Goin M, Giulianelli S, Russo J, Lanari C. Hypermethylation of the progesterone receptor A in constitutive antiprogestin-resistant mouse mammary carcinomas. Breast Cancer Res Treat 2011; 126:319–332.
26. Pompolo S, Pereira A, Kaneko T, Clarke IJ. Seasonal changes in the inputs to gonadotropin-releasing hormone neurons in the ewe brain: an assessment by conventional fluorescence and confocal microscopy. J Neuroendocrinol 2003; 15:538–545.
27. Urbanski HF. Monoclonal antibodies to luteinizing hormone-releasing hormone: production, characterization, and immunocytochemical application. Biol Reprod 1991; 44:681–686.
28. Hagihara K, Hirata S, Osada T, Hirai M, Kato J. Distribution of cells containing progesterone receptor mRNA in the female rat di- and telencephalon: an in situ hybridization study. Mol Brain Res 1992; 14: 239–249.
29. Moffatt CA, Rissman E, Shupnik M, Blaustein JD. Induction of progestin receptors by estradiol in the forebrain of estrogen receptor-α gene-disrupted mice. J Neurosci 1998; 18:9556–9563.
30. Warembourg M, Jolivet A, Milgrom E. Immunohistochemical evidence of the presence of estrogen and progesterone receptors in the same neurons of the guinea pig hypothalamus and preoptic area. Brain Res 1989; 480:1–15.
31. Leranth C, MacLusky NJ, Brown TJ, Chen EC, Redmond DE, Naftolin F. Transmitter content and afferent connections of estrogen-sensitive progestin receptor-containing neurons in the primate hypothalamus. Neuroendocrinology 1992; 55:667–682.
32. Warembourg M, Leroy D, Peytin J, Martinet L. Estrogen receptor and progesterone receptor-immunorreactive cells are not colocalized with gonadotropin-releasing hormone in the brain of the female mink (*Mustela vison*). Cell Tissue Res 1998; 291:33–41.
33. Bayliss DA, Seroogy KB, Millhorn DE. Distribution and regulation by estrogen of progesterone receptor in the hypothalamus of the cat. Endocrinology 1991; 128:2610–2617.
34. Dufourny L, Skinner DC. Influence of estradiol on NADPH diaphorase/ neuronal nitric oxide sintase activity and colocalization with progesterone or type II glucocorticoid receptors in ovine hypothalamus. Biol Reprod 2002; 67:829–836.
35. Foradori CD, Coolen LM, Fitzgerald ME, Skinner DC, Goodman RL, Lehman MN. Colocalization of progesterone receptors in parvicellular dynorphin neurons of the ovine preoptic area and hypothalamus. Endocrionology 2002; 143:4366–4374.
36. Scott CJ, Pereira AM, Rawson JA, Simmons DM, Rossmanith WG, Ing NH, Clarke IJ. The distribution of progesterone receptor (PR) immunoreactivity (-ir) and mRNA in the preoptic area and hypothalamus of the ewe: up-regulation of PR and mRNA in the mediobasal hypothalamus by estrogen. J Neuroendocrinol 2000; 12:565–575.
37. Bethea CL, Fahrenbach WH, Sprangers SA, Freesh F. Immunocytochemical localization of progestin receptors in monkey hypothalamus: effect of estrogen and progestin. Endocrinology 1992; 130:895–905.
38. Mani SK, Blaustein JD. Neural progestin receptors and female sexual behavior. Neuroendocrinology 2012; 96:152–161.
39. Guerra-Araiza C, Amorim MA, Pinto-Almazán R, González-Arenas A, Campos MG, Garcia-Segura LM. Regulation of the phosphoinositide-3 kinase and mitogen-activated protein kinase signaling pathways by progesterone and its reduced metabolites in the rat brain. J Neurosci Res 2009; 87:470–481.
40. Mani SK, Oyola MG. Progesterone signaling mechanisms in brain and behavior. Front Endocrinol 2012; 3:7.
41. Silverman AJ, Witkin JW. Biosynthesis of gonadotropin-releasing hormone during the rat estrous cycle: a cellular analysis. Neuroendocrinology 1994; 59:545–551.
42. Urbanski HF, Doan A, Pierce M. Immunocytochemical investigation of luteinizing hormone-releasing hormone neurons in Syrian hamsters maintained under long or short days. Biol Reprod 1991; 44:687–692.
43. Urbanski HF, Doan A, Pierce M, Fahrenbach WH, Collins PM. Maturation of the hypothalamo-pituitary-gonadal axis of male Syrian hamsters. Biol Reprod 1992; 46:991–996.
44. Silverman AJ, Jhamandas J, Renaud LP. Localization of luteinizing hormone-releasing hormone (LHRH) neurons that project to the median eminence. J Neurosci 1987; 7:2312–2319.
45. Sterling RJ, Gasc JM, Sharp PJ, Tuohimaa P, Baulieu EE. Absence of nuclear progesterone receptor in LH releasing hormone in laying hens. J Endocrionol 1984; 102:R5–R7.
46. Skinner DC, Caraty A, Allingham R. Unmasking the progesterone receptor in the preoptic area and hypothalamus of the ewe: no colocalization with gonadotropin-releasing hormone neurons. Endocrionology 2001; 142:573–579.
47. Weir BJ. The management and breeding of some more hystricomorph rodents. Lab Anim 1970; 4:83–97.
48. King JC, Tai DW, Hanna IK, Pfeiffer A, Haas P, Ronsheim PM, Mitchell SC, Turcotte JC, Blaustein JD. A subgroup of LHRH neurons in guinea pigs with progestin receptors is centrally positioned within the total population of LHRH neurons. Neuroendocrinology 1995; 61:265–275.
49. Denner LA, Weigel NL, Maxwell BL, Schrader WT, O'Malley BW. Regulation of progesterone receptor-mediated transcription by phosphorylation. Science 1990; 250:1740–1743.
50. Power RF, Lydon JP, Conneely OM, O'Malley BW. Dopamine activation of an orphan of the steroid receptor superfamily. Science 1991; 252: 1546–1548.
51. Lethimonier C, Madigou T, Muñoz-Cueto JA, Lareyre JJ, Kah O. Evolutionary aspects of GnRHs, GnRH neuronal systems and GnRH receptors in teleost fish. Gen Comp Endocr 2004; 135:1–16.
52. Millar RP. GnRHs and GnRH receptors. Anim Reprod Sci 2005; 88:5–28.
53. Tsai PS. Gonadotropin-releasing hormone in invertebrates: structure, function, and evolution. Gen Comp Endocrinology 2006; 148:48–53.
54. Tsai PS, Zhang L. The emergence and loss of gonadotropin-releasing hormone in protostomes: orthology, phylogeny, structure and function. Biol Reprod 2008; 79:798–805.
55. Burgus R, Butcher M, Amoss M, Ling N, Monahan M, Rivier J, Fellows R, Blackwell R, Vale W, Guillemin R. Primary structure of ovine luteinizing hormone-releasing factor (LRF). Proc Natl Acad Sci U S A 1972; 69:278–282.
56. King JA, Millar RP. Structure of chicken hypothalamic luteinizing hormone-releasing hormone I. Structural determination on partially purified material. J Biol Chem 1982; 257:10722–10728.
57. Miyamoto K, Hasegawa Y, Nomura M, Igarashi M, Kangawa K, Matsuo H. Identification of the second gonadotropin releasing hormone in chicken hypothalamus: evidence that gonadotropin secretion is probably controlled by two distinct gonadotropin-releasing hormones in avian species. Proc Natl Acad Sci U S A 1984; 81:3874–3878.
58. Jimenez-Liñan M, Rubin BS, King JC. Examination of guinea pig luteinizing hormone-releasing hormone gene reveals a unique decapeptide and existence of two transcripts in the brain. Endocrinology 1997; 138: 4123–4130.
59. Guilgur LG, Ortí G, Strobl-Mazzulla PH, Fernandino JI, Miranda LA, Somoza GM. Characterization of the cDNAs encoding three GnRH forms in the pejerrey fish, *Odontesthes bonariensis* (Atheriniformes) and the evolution of GnRH precursors. J Mol Evol 2007; 64:614–627.
60. An BS, Choi JH, Choi KC, Leung CK. Differential role of progesterone receptor isoforms in the transcriptional regulation of human gonadotropin-releasing hormone I (GnRH I) receptor, GnRH I, and GnRH II. J Clin Endocrinol Metab 2005; 90:1106–1113.
61. Hirshfield AN. Relationship between the supply of primordial follicles and the onset of follicular growth in rats. Biol Reprod 1994; 50:421–428.